Mannose 6 phosphorylation of lysosomal enzymes controls B cell functions

Takanobu Otomo,[1,2] Michaela Schweizer,[3] Katrin Kollmann,[1] Valéa Schumacher,[4] Nicole Muschol,[1] Eva Tolosa,[4] Hans-Willi Mittrücker,[4] and Thomas Braulke[1]

[1]Department of Biochemistry, Children's Hospital; [3]Department of Electron Microscopy, Center for Molecular Neurobiology; and [4]Department of Immunology, University Medical Center Hamburg-Eppendorf, 20246 Hamburg, Germany
[2]Department of Pediatrics, Osaka University Graduate School of Medicine, 5650871 Suita, Osaka, Japan

Antigen processing and presentation and cytotoxic targeting depend on the activities of several lysosomal enzymes that require mannose 6-phosphate (M6P) sorting signals for efficient intracellular transport and localization. In this paper, we show that mice deficient in the formation of M6P residues exhibit significant loss of cathepsin proteases in B cells, leading to lysosomal dysfunction with accumulation of storage material, impaired antigen processing and presentation, and subsequent defects in B cell maturation and antibody production. The targeting of lysosomal and granular enzymes lacking M6P residues is less affected in dendritic cells and T cells and sufficient for maintenance of degradative and lytic functions. M6P deficiency also impairs serum immunoglobulin levels and antibody responses to vaccination in patients. Our data demonstrate the critical role of M6P-dependent transport routes for B cell functions in vivo and humoral immunity in mice and human.

Introduction

Lysosomes function in the degradation of macromolecules delivered by the biosynthetic, endocytic, or autophagic pathway and depend on the concerted action of ∼60 lysosomal enzymes at low pH (Saftig and Klumperman, 2009; Schröder et al., 2010). Newly synthesized lysosomal hydrolases are modified on their N-linked oligosaccharides with mannose 6-phosphate (M6P) residues, which can be recognized by M6P-specific receptors in late Golgi compartments mediating their segregation from the secretory pathway and delivery to endosomal/lysosomal structures (Braulke and Bonifacino, 2009). The key enzyme in the formation of M6P residues is the *N*-acetylglucosamine-1-phosphotransferase complex consisting of three subunits that are encoded by two genes, *GNPTAB* and *GNPTG* (Reitman et al., 1981; Waheed et al., 1981; Bao et al., 1996; Raas-Rothschild et al., 2000; Kudo et al., 2005; Tiede et al., 2005). The loss of phosphotransferase activity in individuals with mucolipidosis II (MLII or I-cell disease), a rare lysosomal storage disease with an incidence of 1:650,000, prevents the formation of the M6P recognition marker, which subsequently leads to missorting and hypersecretion of multiple lysosomal enzymes associated with lysosomal dysfunction and accumulation of nondegraded material (Braulke et al., 2013). However, in certain cell types in MLII patients such as hepatocytes, Kupffer cells, or cytolytic lymphocytes, the absence of lysosomal storage material and nearly normal level of selected lysosomal enzymes were observed, suggesting the existence of alternate M6P-independent targeting pathways (Owada and Neufeld, 1982; Waheed et al., 1982; Griffiths and Isaaz, 1993; Glickman and Kornfeld, 1993). Data on the direct consequences of variable targeting efficiency of nonphosphorylated lysosomal enzymes on cell functions in vivo are lacking.

Previous mouse studies have demonstrated that in antigen-presenting cells several lysosomal enzymes, in particular cathepsin proteases, are implicated in the limited degradation of proteins destined for the major histocompatibility complex (MHC) class II processing pathway. Furthermore, cathepsins have been shown to be involved in the stepwise proteolytic removal of CD74 (invariant chain), which regulates the assembly,

Correspondence to Takanobu Otomo: otomo@ped.med.osaka-u.ac.jp; or Thomas Braulke: braulke@uke.de

T. Otomo's present address is Department of Genetics, Osaka University Graduate School of Medicine, 5650871 Suita, Osaka, Japan.

Abbreviations used in this paper: αFuc, α-fucosidase; αMan, α-mannosidase; βGal, β-galactosidase; βHex, β-hexosaminidase; CFSE, carboxyfluorescein succinimidyl ester; Cts, cathepsin; DC, dendritic cell; Lamp1, lysosome-associated membrane protein 1; LPS, lipopolysaccharide; M6P, mannose 6-phosphate; MFI, mean fluorescence intensity; MHC, major histocompatibility complex; MLII, mucolipidosis II; OT-II, Ova-specific T cell receptor transgenic mice; Ova, ovalbumin; WT, wild-type.

The Rockefeller University Press $30.00
J. Cell Biol. Vol. 208 No. 2 171–180
www.jcb.org/cgi/doi/10.1083/jcb.201407077

peptide loading, and export of MHC II molecules for recognition by CD4 T cells (Riese et al., 1998; Driessen et al., 1999; Nakagawa et al., 1998, 1999; Honey and Rudensky, 2003).

To examine the significance of variable targeting efficiencies of lysosomal enzymes in the absence of phosphotransferase activity on cells of the immune system in vivo, *Gnptab* knock-in mice (MLII mice) were analyzed. These mice mimic the clinical symptoms of MLII patients (Kollmann et al., 2012, 2013) and we find that the levels of lysosomal proteases are severely decreased in MLII B cells and impair the proliferation, differentiation, and antigen presentation as well as their interaction with T helper cells, resulting in reduced immunoglobulin production. Compared with MLII B cells, MLII T and dendritic cells (DCs) maintained higher lysosomal protease activities, and their cell functions were only moderately affected. Importantly, defective humoral immunity was also observed in MLII patients.

Results and discussion

Missorting of lysosomal proteases causes accumulation of storage material in B cells

In B cells of MLII mice, a profound and specific reduction (<10% of wild-type [WT]) of lysosomal protease activities, namely of cathepsin B (CtsB) and CtsL (Fig. 1 A), and a complete loss of immunoreactive CtsZ and CtsS were observed (Fig. 1 B). In contrast, activities of β-hexosaminidase (βHex), β-galactosidase (βGal), α-fucosidase (αFuc), and α-mannosidase (αMan), all involved in lysosomal degradation of oligosaccharides, were not or only moderately reduced in B cells of MLII mice (Fig. 1 A) or in B lymphoblasts of MLII patients (Little et al., 1987; Tsuji et al., 1988; Glickman and Kornfeld, 1993). The higher amounts of the lysosome-associated membrane protein 1 (Lamp1) in MLII B cells indicated an increased number and/or size of lysosomes most likely because of storage material (Karageorgos et al., 1997; Kollmann et al., 2012). Indeed, ultrastructural analysis showed a high number of both electron-lucent vacuoles and multi-lamellar bodies representing heterogeneous accumulation of storage material in 42% of MLII B cells, which was absent in WT B cells (Fig. 1 C). Compared with MLII B cells, MLII T cells showed higher residual enzyme activities of CtsB and CtsL (∼20% of WT), and CtsZ immunoreactivity was still detectable (Fig. 1, D and E). Activities of lysosomal glycosidases βGal, αFuc, and αMan were only marginally reduced in MLII T cells (>50% residual activity compared with WT T cells), and βHex was not changed at all (Fig. 1 D). No lysosomal storage vacuoles could be detected by transmission EM in splenic CD4 (Fig. 1 F) or CD8 (Fig. 1 G) MLII T cells. The partial loss of lysosomal enzymes did not reveal any statistically significant effects on the splenic immune cell composition in MLII mice (Fig. S1). In previous studies on cytotoxic lymphocytes of MLII patients a reduction of βHex activity to 30% of control has been observed (Griffiths and Isaaz, 1993). Our data on MLII T cells are in agreement with numerous other studies that 5–10% of normal activity of single lysosomal enzymes is sufficient to maintain their function in lysosomes and prevent the accumulation of storage material (Fratantoni et al., 1969; Sawkar et al., 2006). Furthermore, these data suggest the existence of M6P-independent transport routes for distinct lysosomal/granule enzymes, which appear to be sufficient for maintaining degradative lysosomal and lytic granule functions, e.g., in MLII T cells.

Antigen fragmentation and presentation is affected in M6P-deficient B cells

In professional antigen-presenting cells, lysosomal proteases are required for the degradation of antigenic proteins in the endosomal pathway and processing of CD74 (invariant chain), which prevents in its intact form premature loading of peptides to MHC II molecules (Honey and Rudensky, 2003). The antigen–MHC II complexes are subsequently transported to the cell surface and presented to CD4 T cells. DC–T cell interactions are essential for T cell priming, and B cell–T cell interactions are crucial for B cell differentiation after activation. We undertook several experimental approaches to examine the impact of variable missorting of lysosomal enzymes in MLII B cells and DCs on antigen presentation to CD4 T cells. First, we investigated antigen uptake by B cells and DCs. Cells were incubated with fluorochrome-conjugated ovalbumin (Ova) protein and subsequently analyzed by flow cytometry. After 20-min incubation with Alexa Fluor 647–Ova, similar intracellular fluorescence intensities were observed in WT and MLII B cells and DCs (Fig. 2 A), indicating comparable rates of antigen uptake. Next, we studied the antigen degradation by incubating cells with DQ-Ova, which releases the DQ-fluorophore upon lysosomal proteolysis of Ova. After the 20-min loading period, a linear increase in the fluorescence intensity was observed in WT B cells reaching a plateau after 90 min (Fig. 2 B). In contrast, no increase in fluorescence intensity was detectable in MLII B cells. Compared with B cells, both WT and MLII DCs display a similar time course of increasing fluorescence intensity with slightly reduced rates of Ova proteolysis in MLII DCs (Fig. 2 B). Thus, MLII and WT antigen-presenting cells were similarly efficient in protein uptake. However, MLII B cells, but not MLII DCs, were profoundly impaired in proteolytic degradation of the endocytosed Ova protein.

In both MLII B cells and DCs, we observed an accumulation of intermediate CD74 degradation fragments (Fig. 2 C), which most likely prevent MHC II loading with antigenic peptides (Roche and Cresswell, 1991). Proteolytic cleavage of CD74 depends on CtsS. At steady state, MLII DCs maintained higher amounts of CtsS protein (∼38% of WT DCs) than MLII B cells (∼5% of WT B cells), which might restrict accumulation of CD74 degradation intermediates in MLII DCs. Furthermore, the total level of MHC II molecules at the surface of activated B cells from MLII mice was reduced to 58% of WT B cells (Fig. 2 D). This might be the consequence of ubiquitination with chains of distinct length, which is a prerequisite for the subsequent degradation of internalized surface MHC II (Ma et al., 2012; Furuta et al., 2013) in MLII B cells. EM analysis of MLII DCs revealed no changes in morphology (Fig. 2 E), and the lack of lysosomal storage material suggests that residual lysosomal enzyme activities are sufficient for maintaining cellular homeostasis. Furthermore, MLII DCs fail to exhibit severe antigen degradation defects. This might be explained by

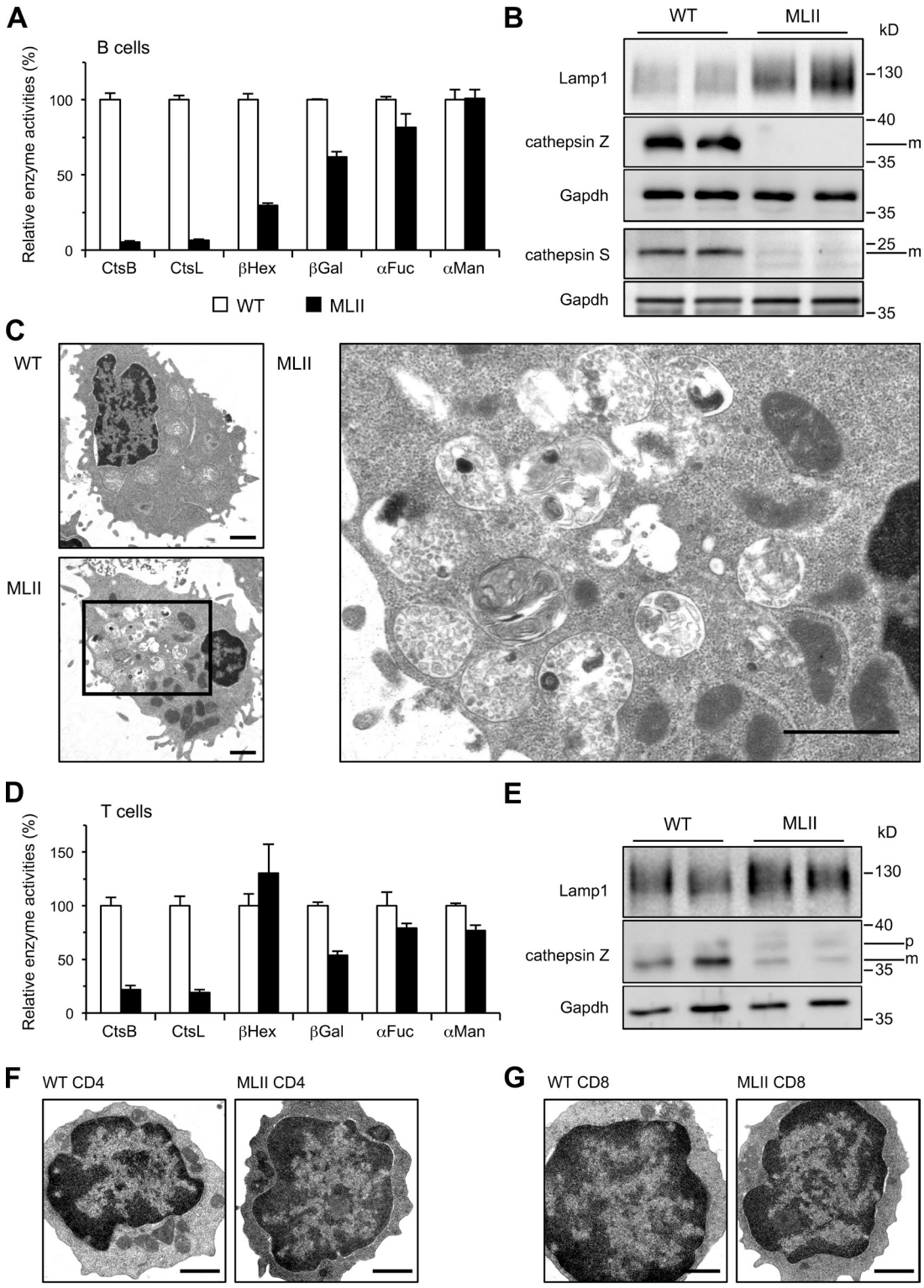

Figure 1. **Loss of lysosomal proteases and accumulation of storage material in B cells from MLII mice.** (A) The activities of CtsB, CtsL, βHex, βGal, αFuc, and αMan in extracts of B cell blasts. Specific activities in B cells of WT mice were set to 100%. Mean and SEM (n = 3–6). (B) Western blot from B cell extracts. (C) Electron micrographs of splenic B cell blasts revealed accumulation of lysosomal storage material in MLII cells. Higher magnification of indicated area from a representative MLII B cell is shown. Bars, 1 µm. (D) Relative activities of CtsB, CtsL, βHex, βGal, αFuc, and αMan in extracts of T cell blasts (percentage of WT controls). Mean and SEM (n = 3–6). (E) Western blot from T cell extracts. m, mature form; p, precursor form. (F and G) Electron micrographs of purified splenic MLII CD4 T cells (F) and CD8 T cells (G) revealed normal appearance. Bars, 1 µm.

the relatively high residual expression of CtsS and most likely other acid proteases, as compared with B cells, which allow rather normal degradation of the indicator antigen DQ-Ova and partial proteolytic processing of CD74.

To directly measure antigen presentation to CD4 T cells in vitro, activated B cells were incubated with Ova protein for 2 h, washed, and then cultured for 4 d with Ova-specific CD4 T cells obtained from Ova-specific T cell receptor transgenic mice

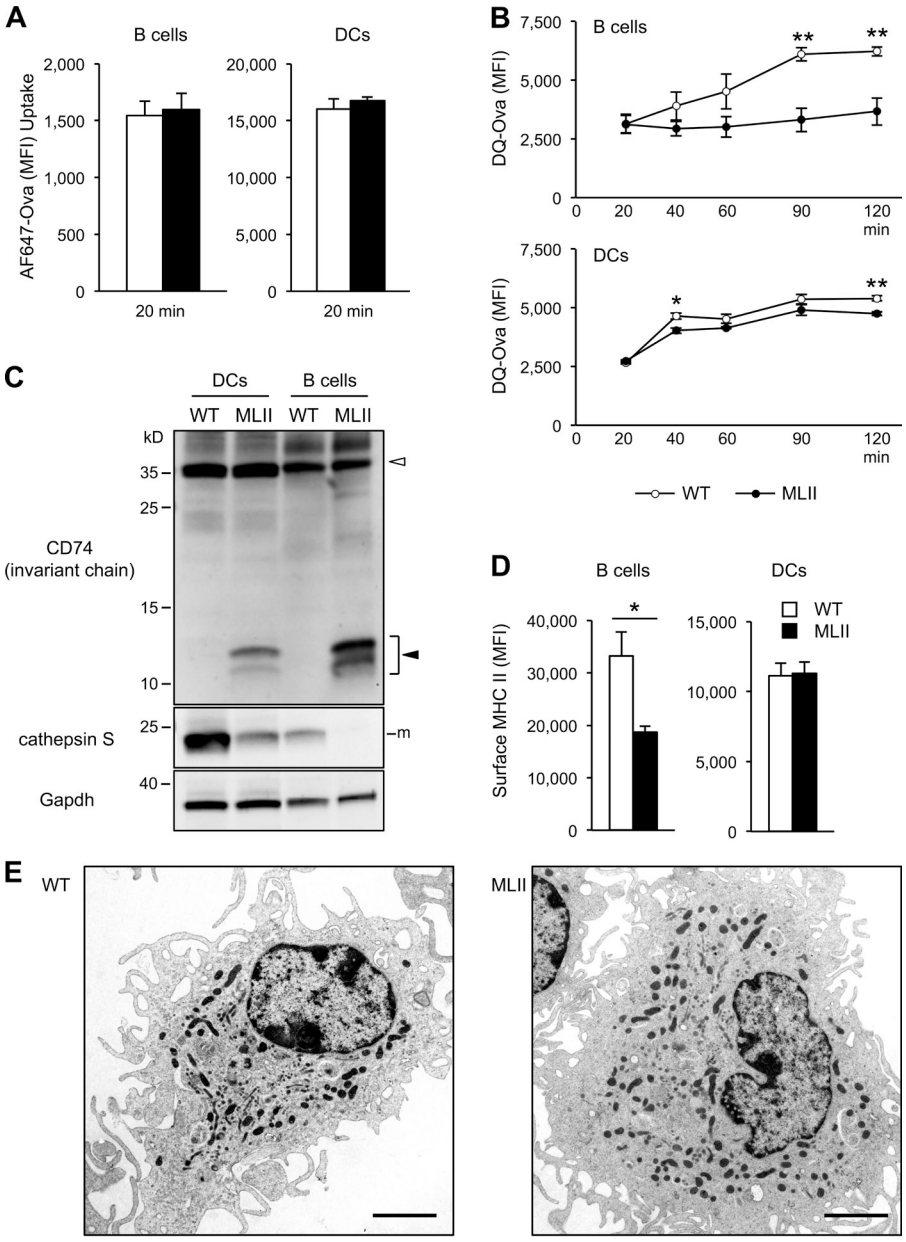

Figure 2. **Cathepsin deficiencies impair antigen and CD74 degradation in antigen-presenting cells from MLII mice.** (A) Uptake of Alexa Fluor 647 (AF647)–Ova in WT and MLII B cells and DCs for 20 min. (B) Fragmentation of DQ-Ova antigen in B cells and DCs. After uptake the proteolytic release of DQ fluorescence was quantified over time. (C) Representative CD74 and CtsS Western blot from WT and MLII B cells and DCs. Positions of full-length CD74 (open arrowhead) and of accumulating CD74 degradation intermediates (closed arrowhead) are indicated. m, mature form. (D) Total surface MHC II level on B cells and DCs analyzed by flow cytometry. Mean and SEM ($n = 3$). *, $P < 0.05$; **, $P < 0.01$. (E) Electron micrographs of MLII DCs revealed normal appearance. Bars, 2.5 µm.

(OT-II; Barnden et al., 1998). Presentation of Ova peptides by B cells induced the activation and proliferation of OT-II cells, which was dependent on the number of B cells, and the concentration of Ova used for loading of B cells (Fig. 3 A). Ova-loaded MLII B cells induced significantly less proliferation of OT-II cells than WT B cells, indicating impaired antigen presentation by MLII B cells. The proliferation of OT-II cells was also affected when MLII B cells were preincubated with the cognate Ova peptide (Fig. 3 B). Furthermore, this effect could not be rescued with high peptide doses, supporting our observation of reduced MHC II level at the surface of MLII B cells. Because presentation of peptides does not require proteolytic fragmentation, missorting of lysosomal enzymes appears to impede additional steps in the presentation pathway, such as peptide loading of MHC II or MHC II distribution, and thereby further restricts CD4 T cell activation by B cells.

Incubation of Ova-loaded WT B cells with OT-II T cells also caused further maturation and the acquisition of the plasma cell marker CD138 by WT B cells (Fig. 3, C and D). In contrast, there was reduced expression of CD138 both in terms of frequency of positive cells and expression level per cell (mean fluorescence intensity [MFI]) on the surface of MLII B cells, indicating that defects in antigen presentation in MLII B cells result in restricted cooperation with T cells and lead to reduced B cell maturation. Defects in antigen degradation and presentation can be easily explained by the low abundance of the lysosomal proteases CtsL, CtsS, and CtsZ, and most likely also of the disulfide bond cleaving γ-interferon–inducible lysosomal thiolreductase in MLII B cells, because mice deficient in these enzymes show impaired MHC II–restricted antigen presentation (Nakagawa et al., 1998, 1999; Driessen et al., 1999; Maric et al., 2001; Honey and

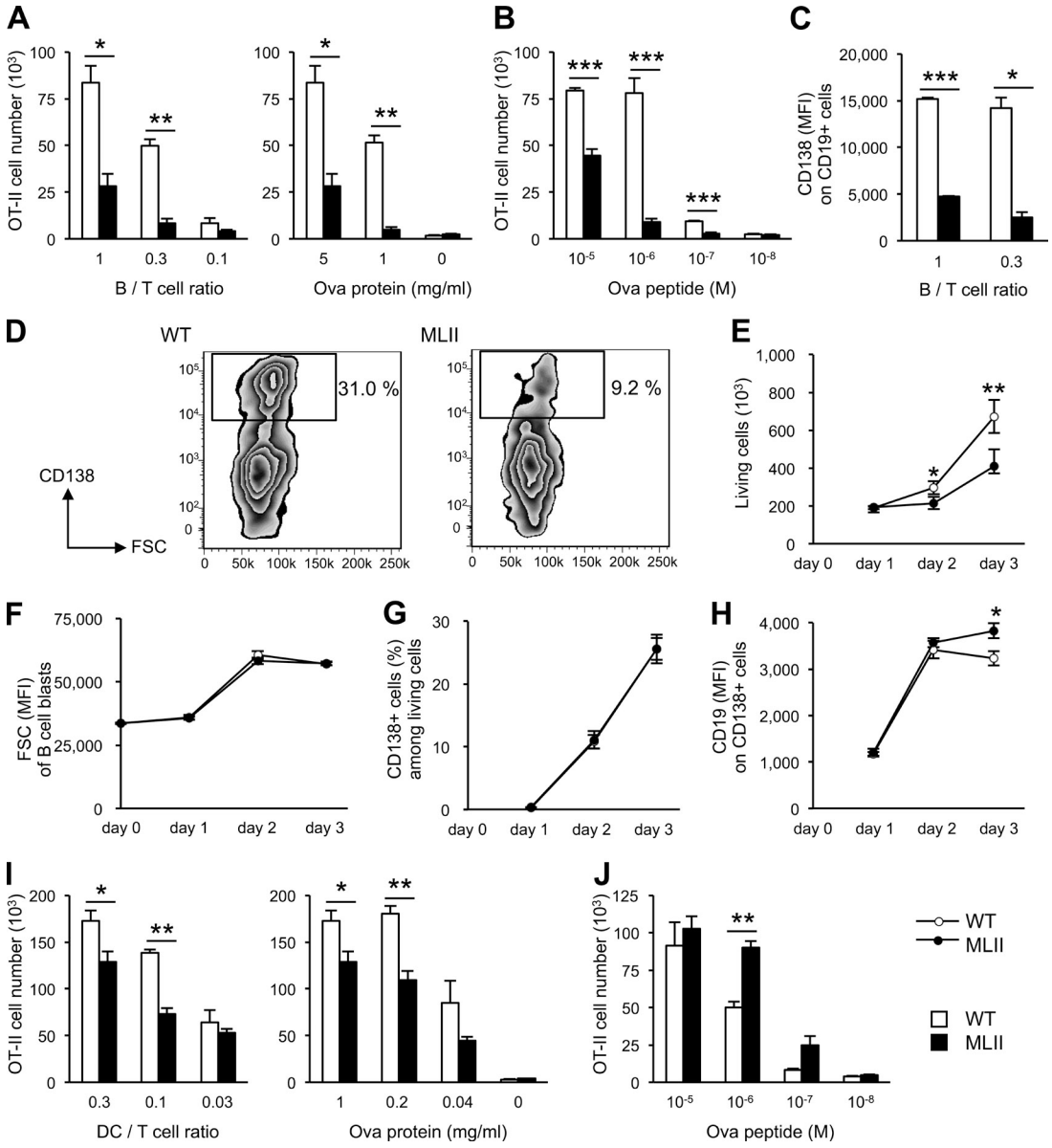

Figure 3. **Defective antigen presentation, proliferation, and differentiation of MLII B cells.** (A) Antigen presentation by B cells to Ova-specific CD4 T cells. T cell responses upon loading of B cells with Ova (5 mg/ml) at different B/T cell ratios and loading with different amounts of Ova protein at fixed B/T ratio (1:1) are shown. (B) CD4 T cell response to B cells loaded with Ova peptide at fixed B/T ratio (1:1). (C and D) Impaired differentiation of MLII B cells. (C) Ova antigen presentation test was performed and plasma cell marker CD138 expression on CD19-positive B cells was quantified by flow cytometry. (D) MFI values of CD138 on CD19-positive cells (B/T ratio of 1:0.3) and zebra plots of CD19-positive cells (B/T ratio of 1) are shown. Rectangles indicate region and percentage of differentiated plasmablasts. (E–H) T cell–independent proliferation and differentiation of B cells in vitro. Purified splenic B cells (10^6) from WT and MLII mice were stimulated with 10 µg/ml LPS and analyzed by flow cytometry at the indicated time. Proliferation of B cells (E), blast formation of B cells determined by forward scatter (FSC; F), percentages of B cells that acquired the plasma cell marker CD138 (G), and MFI of CD19 on CD138-positive cells (H) are shown. (I) T cell responses upon loading of DCs with Ova protein (1 mg/ml) at different DC/T cell ratios and loading with different amounts of Ova protein at fixed DC/T ratio (0.3:1) are shown. (J) CD4 T cell response to DCs loaded with Ova peptide at fixed DC/T ratio (0.3:1). Mean and SEM of three to six experiments. *, $P < 0.05$; **, $P < 0.01$; ***, $P < 0.001$.

Rudensky, 2003). The presence of lysosomal storage material, however, might also contribute to abnormal B cell functions, similarly to dysfunctional MLII osteoblasts and chondrocytes (Kollmann et al., 2013).

MLII DCs were also tested for their capacity to present antigen to CD4 T cells. MLII DCs displayed some reduction in Ova protein presentation to T cells (Fig. 3 I); however, this impairment was far less profound than the defect observed in MLII B cells. Peptide presentation by MLII DCs was similar or even slightly higher than that by WT DCs (Fig. 3 J), indicating that the DCs are not generally deficient in activation of T cells. It has been shown that DCs and B cells require a closely defined range of protease activities that, on one hand, generate peptides for presentation and, on the other hand, do not lead to the complete degradation of antigens (Delamarre et al., 2005, 2006). Our data suggest that the lysosomal proteolytic capacity of MLII DCs is still within this range and therefore allows generation of antigenic peptides, although at reduced levels.

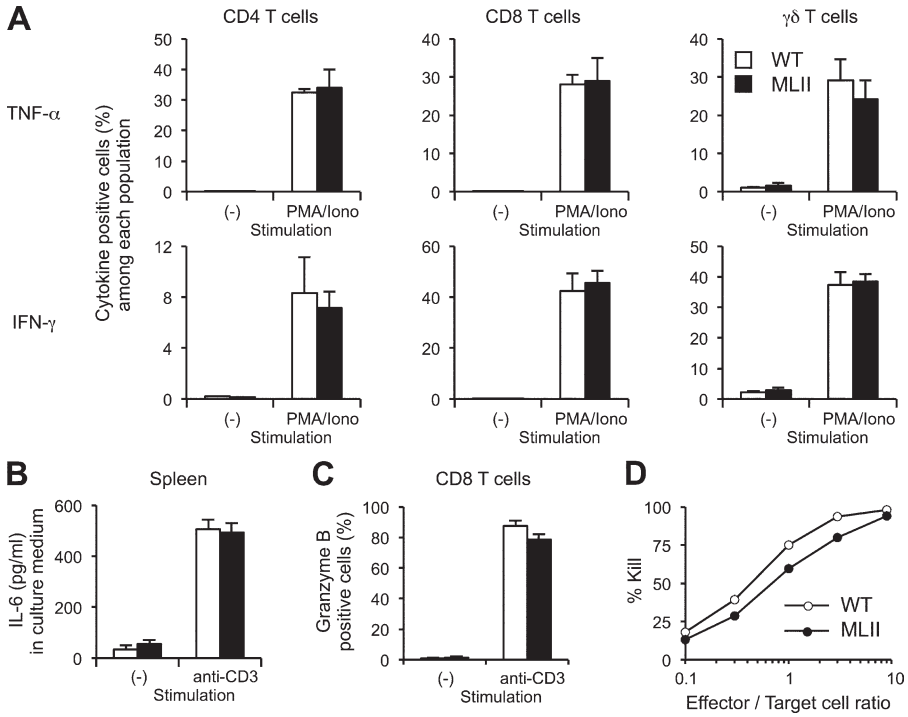

Figure 4. **Functionally intact MLII T cells.** (A) Normal TNF and IFN-γ production by CD4, CD8, and γδ T cells. Spleen cells from mice were stimulated with phorbol 12-myristate 13-acetate and ionomycin (PMA/Iono) in the presence of brefeldin A. After fixation and permeabilization, intracellular TNF and IFN-γ were quantified by flow cytometry. (B) Comparable production of IL-6. Spleen cells (4×10^5 cells per well) from mice were stimulated with anti-CD3 mAb. After 24 h, culture supernatant was collected and IL-6 was quantified by ELISA. (C) Granzyme B production by CD8 T cells after stimulation with anti-CD3 mAb for 3 d. The data are expressed as mean and SEM of three to four experiments. (D) Normal cytotoxic functions of MLII CD8 T cells. Spleen cells from WT and MLII mice (H-2^b) were stimulated with irradiated spleen cells from BALB/c mice (H-2^d) in the presence of IL-2 (10 U/ml). After 5 d, living cells (effectors) were purified and mixed with CFSE-labeled A20 cells (H-2^d; targets) for 4 h in different ratios. Survival of A20 cells was measured by flow cytometry, and percentage of killing is shown. The data shown are from a single representative experiment out of three repeats. Mean is shown; $n = 2$.

In contrast, the missorting of lysosomal proteases in MLII B cells is more substantial with only very limited lysosomal proteolysis of antigens. The results further imply that DCs and B cells differentially rely on M6P-independent targeting pathways for individual lysosomal hydrolases.

Proliferation and differentiation of MLII B cells is impaired upon T cell–independent stimulation

To analyze whether dysfunctional lysosomes impair proliferation and differentiation of B cells, we stimulated purified B cells in a T cell–independent manner with lipopolysaccharide (LPS; Fairfax et al., 2008). After stimulation for 3 d, proliferation of MLII B cells was reduced by 50% compared with WT cells (Fig. 3 E). In response to LPS stimulation, both WT and MLII B cells showed similar blast formation rates, as determined by the increase in size (Fig. 3 F) and surface expression of the plasmablast marker CD138 (Fig. 3 G). However, on day 3 of activation, we observed a significant decrease in the surface expression level (MFI) of CD19 on CD138-positive cells from WT but not MLII B cells (Fig. 3 H). Because the B cell marker CD19 is down-regulated during differentiation of B cells into plasmablasts and plasma cells (Fairfax et al., 2008), our data suggest an impaired terminal differentiation of MLII B cells. Although the molecular mechanisms of CD19 down-regulation are unknown, it cannot be excluded that defects in lysosomal degradation affect endocytosis and distribution of CD19 in MLII B cells.

Residual lysosomal enzyme activities allow maintenance of T cell functions

We next investigated the function of MLII T cells. To examine the capability of T cells to respond to stimuli, spleen cells were incubated with phorbol 12-myristate 13-acetate and ionomycin. Secretion of cytokines was blocked with brefeldin A (Donaldson et al., 1992) and the intracellular accumulation of TNF and IFN-γ in CD4, CD8, and γδ T cells was analyzed by flow cytometry. The extent of TNF and IFN-γ response after activation was similar in WT and MLII T cell populations (Fig. 4 A). In addition, when spleen cells were stimulated with anti-CD3 mAb, similar amounts of IL-6 were secreted by WT and MLII cells (Fig. 4 B).

To examine the function of cytotoxic T cells derived from MLII mice, spleen cells were stimulated with anti-CD3 mAb for 3 d and the accumulation of granzyme B in CD8 T cells was analyzed by flow cytometry. Similar amounts of granzyme B were found in MLII and WT CD8 T cells (Fig. 4 C). When CD8 T cells from WT and MLII mice were incubated with allogeneic spleen cells, a comparable killing ability of allogeneic target cells was observed for WT and MLII cytotoxic T cells (Fig. 4 D). These findings are in agreement with conserved cytotoxicity of T cells from MLII patients, although these cells showed diminished levels of granzyme A and B when compared with control levels (Griffiths and Isaaz, 1993). The data suggest that the loss of M6P residues on lysosomal and granular enzymes and their subsequent missorting in MLII T cells can be partially compensated by alternative lysosomal targeting pathways that allow maintenance of central T cell functions such as cytokine production and cytotoxicity.

Impaired antibody response in MLII

To examine the biological significance of impaired homeostasis of lysosomes in B cells, the immune status of MLII mice in vivo was studied. Sera from MLII mice showed normal

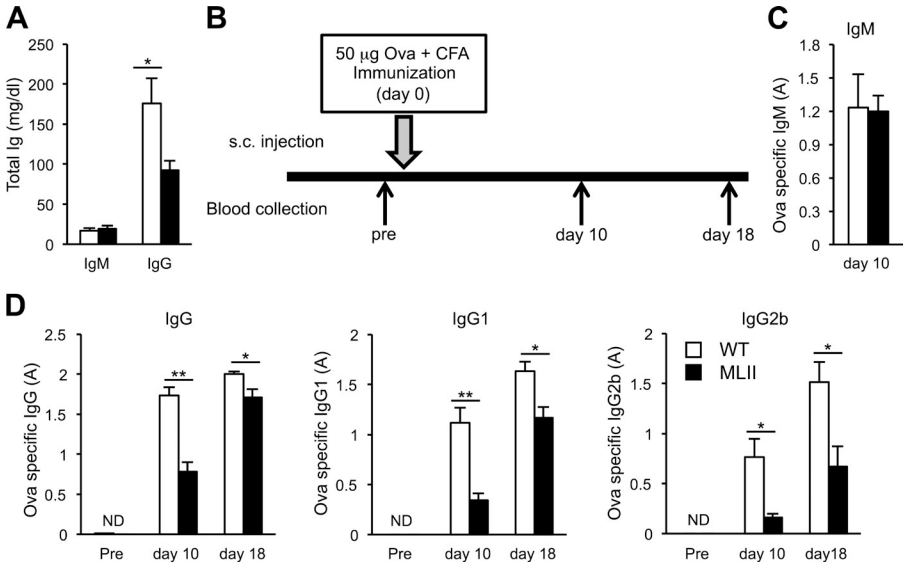

Figure 5. **Impaired antibody production in MLII mice.** (A) Basal total IgM and IgG concentrations were determined in serum from WT and MLII mice. (B) Scheme of subcutaneous (s.c.) vaccination using 50 µg of Ova with complete Freund's adjuvant (CFA) and blood analyses. (C and D) Ova-specific immunoglobulin titers were determined in mouse serum prior (pre) and on days 10 and 18 after immunization. Ova-specific IgM titers (C) and Ova-specific IgG, IgG1, and IgG2b (D) were determined by ELISA. The data are expressed as mean and SEM of five to seven experiments. A, absorbance units; ND, not detectable; *, $P < 0.05$; **, $P < 0.01$.

serum levels of IgM but significantly reduced IgG (Fig. 5 A). Upon subcutaneous immunization with Ova in complete Freund's adjuvant (Fig. 5 B), we found similar serum levels of Ova-specific IgM in MLII and WT mice 10 d after immunization (Fig. 5 C). However, Ova-specific total IgG, IgG1, and IgG2 were significantly reduced in MLII mice at days 10 and 18 after immunization (Fig. 5 D). Histochemically, no differences in splenic germinal center formation could be observed between WT and MLII mice.

To determine whether alterations in B cell functions in MLII mice are relevant for human disease, the immune status of four MLII patients was analyzed. Normal blood cell counts, including the numbers of leukocytes, erythrocytes, and platelets, have been reported in the medical records of four MLII patients. However, when we analyzed fresh blood samples from two patients for the distribution of different lymphocyte subsets by flow cytometry, we noticed a decreased percentage of B cells and an increased percentage of T cells compared with the age-matched reference range (Table S1; Comans-Bitter et al., 1997). When the B cell subset composition of the 2.4-yr-old female MLII patient 3 was analyzed further by flow cytometry, she exhibited a high percentage of naive B cells (identified as $CD27^{-}IgD^{+}$), whereas the relative proportion of memory B cells ($CD27^{+}$), including the cells that underwent class switching, were reduced in comparison with age-matched reference ranges (Table S1; Morbach et al., 2010). Examination of serum immunoglobulins revealed low concentrations of total IgG, IgA, and IgM in MLII patients compared with the age-matched reference range (Table S2; Stiehm and Fudenberg, 1966), with the exception of patients 1 and 2 who showed normal IgG levels caused by intravenous injection of immunoglobulin preparations to prevent common infections. Most importantly, the specific antibody response to vaccination was poor or not detectable in all MLII patients (Table S2), which is consistent with MLII mouse data. The low level of memory B cells in the patient analysis indicates impaired B cell maturation in response to antigen and defective immunoglobulin class switch, altogether preventing an effective response against pathogens.

There are only few studies that report on B cell function in lysosomal storage disorders. Kojima et al. (1979) described an MLII patient with a low number of B cells, but normal immunoglobulin concentrations; however, they did not provide data on the underlying mechanisms. Patients with α-mannosidosis also showed low IgG and weak response to vaccinations (Desnick et al., 1976; Malm et al., 2000). Interestingly, lymphocytes from α-mannosidosis patients were filled with storage material that could impair antigen processing and presentation by these cells. The cause of the defects in B cell response is unclear and might be different to MLII because we observe normal αMan activity in MLII B cells. Studies on mice defective in the lysosomal degradation of glycosaminoglycans have led to the speculation that the accumulating negatively charged glycosaminoglycans affect lysosomal function or directly impact lysosomal enzyme activities or peptide loading to MHC II molecules (Daly et al., 2000). The identity of storage material in MLII B cells is unknown; however, our results do not exclude that accumulated storage materials observed in MLII B cells could affect general lysosomal functions and primarily or secondarily impair antigen presentation as well as antibody production. Although airway obstruction caused by skeletal deformities, enlarged tongue, thickened mucosa, and larynx alterations are believed to be responsible for the recurrent infections in MLII (Peters et al., 1985), the data shown here indicate that the functionally impaired immune system contributes to the high predisposition to infections in MLII patients.

The data presented here demonstrated the biological significance of M6P-independent targeting pathways in vivo allowing the transport of lysosomal hydrolases lacking M6P residues in sufficient amounts to maintain almost normal DC and T cell functions. In contrast, the missorting of subsets of non-M6P–modified enzymes, in particular cathepsin proteases, severely impairs antigen fragmentation and presentation in B cells and DCs as well as B cell maturation and the subsequent immune status in mice and patients with MLII.

Materials and methods

Human

MLII patients' data were collected from their medical record under the written informed parent's consent according to the Declaration of Helsinki. Patient 1 and 2 were of Japanese, patient 3 of German, and patient 4 of Portuguese origin. The study was approved by the medical ethics committee of the Ärztekammer Hamburg. Genomic DNA was extracted from patients' skin fibroblasts or lymphocytes, and individual exons and adjacent intronic regions of *GNPTAB* were amplified with primers previously published (Tiede et al., 2005; Otomo et al., 2009) followed by standard BigDye sequencing protocol (Applied Biosystems).

Mouse strains

A knock-in mouse model for MLII was generated by the insertion of a cytosine at position c.3082 in exon-16 of the mouse *Gnptab* gene (*Gnptab*$^{c.3082insC}$) that caused a premature translational termination leading to a truncated phosphotransferase protein (p.G1028R*fs*X16; Kollmann et al., 2012). This mutation corresponds to a mutation, c.3145insC, identified in an MLII patient (Tiede et al., 2005). For the experiments, age- (between 8 and 15 wk) and gender-matched mice were used. WT littermates served as controls. OT-II mice are transgenic for an αβ T cell receptor specific for chicken Ova in the context of MHC class II (I-A^b; Barnden et al., 1998). MLII mice and OT-II mice were bred under specific-pathogen–free conditions at the animal facility of the University Medical Center Hamburg-Eppendorf. Experiments were conducted according to German animal protection law.

Isolation and culture of immune cells from mouse

Immune cells were isolated from spleen by passing through a 200-µm metal sieve and 70-µm cell strainer into 10 mM PBS, pH 7.4. Subsequently, red blood cells were lysed with ACK lysing buffer (155 mM NH_4Cl, 10 mM $KHCO_3$, and 100 µM EDTA, pH 7.2). The remaining immune cells were used for further analysis including flow cytometry, activation, and cultivation. Cells were cultured with complete medium (RPMI1640 medium supplemented with 5% heat-inactivated FCS, 2 mM L-glutamine, 50 µM β-mercaptoethanol, and 50 µg/ml gentamycin). B and T cell blasts were obtained by stimulation with 10 µg/ml LPS (Sigma-Aldrich) or hamster anti–mouse CD3ε mAb (145-2C11; 1 µg/ml) + IL-2 (10 U/ml; PROLEUKIN S; Novartis), respectively. For the magnetic bead–based purification of B and T cells, we used MACS cell separation (Miltenyi Biotec) according to the manufacturer's protocol. Positive purification of B cells was done with FITC-conjugated rat anti–mouse CD19 mAb (1D3) followed by anti-FITC microbeads (Miltenyi Biotec). Negative purification of CD4 T cells was done with a cocktail of FITC-conjugated rat anti–mouse CD8 (53-6.7), rat anti–mouse CD11b (M1/70), rat anti–mouse CD19 (1D3), rat anti–mouse F4/80 (BM8), and mouse anti–rat MHC II (OX-6) mAbs followed by anti-FITC microbeads. DCs were derived by culturing bone marrow cells with BMDC medium (RPMI1640 medium supplemented with 10% heat-inactivated FCS, 2 mM L-glutamine, 1 mM sodium pyruvate, 50 µM β-mercaptoethanol, 50 µg/ml gentamycin, and 20ng/ml recombinant murine GM-CSF [PeproTech]) for 8 d (Inaba et al., 2009). BMDC medium was replaced on day 3 and 6. For functional assays, the cell plates were rinsed to harvest nonadherent cells. DCs were CD11c+ and >80% MHC II+.

Antibodies for flow cytometry

For the analysis of mouse samples, we used hamster anti–mouse CD3 (500A2); rat anti–mouse CD4 (RM4-5); rat anti–mouse CD8a (53–6.7); rat anti–mouse CD11b (M1/70); hamster anti–mouse CD11c (N418); rat anti–mouse CD19 (1D3); rat anti–mouse CD138 (281–2); rat anti–mouse Gr1 (RB6-8C5); rat anti–mouse Ly6C (AL-21); hamster anti–mouse γδ T cell receptor (GL3); rat anti–mouse MHC II (M5/114.15.2); rat anti–mouse TNF (MP6-XT22); rat anti–mouse IFN-γ (XMG1.2); mouse anti–human granzyme B (GB12); and rat anti–mouse FoxP3 (FJK-16S). For the analysis of human blood, we used mouse anti–human CD3 (OKT3); mouse anti–human CD4 (RPA-T4); mouse anti–human CD8a (RPA-T8); mouse anti–human CD19 (HIB19); mouse anti–human CD27 (O323); mouse anti–human CD45 (HI30); mouse anti–human CD56 (N901 [NKH-1]); and mouse anti–human IgD (IA6-2). All antibodies used for flow cytometry and purification of cells were purchased from BD, BioLegend, or eBioscience.

Flow cytometry for mouse cells

After preparation, surface staining of the immune cells was performed with fluorochrome or biotin-conjugated mAb for 20 min on ice. Dead cells were stained with Pacific orange succinimidyl ester (Life technologies). Cells were fixed with PBS with 2% PFA for 20 min at RT. Intracellular staining was performed with fluorochrome-conjugated mAb for 20 min at RT in permeabilization buffer (PBS, 0.3% saponin, and 0.1% BSA). Intranuclear staining of FoxP3 was performed using FoxP3 fixation/permeabilization reagents (eBioscience) according to the manufacturer's protocol with fluorochrome-conjugated anti-FoxP3 antibody. After staining, cells were measured on a Canto II flow cytometer (BD) and data were analyzed using the FACS Diva software (BD) and FlowJo (Tree Star).

Flow cytometry for human blood

50 µl of freshly drawn blood were stained with cocktails of antibodies designed to identify the main leukocyte subsets and the B cell subpopulations. After 30-min incubation with the antibody cocktails, erythrocytes were lysed using the BD Lysing Solution (BD) and the remaining cells were washed, resuspended in FACS buffer, and analyzed using a FACS Canto (BD). Data were acquired and analyzed using the FACS Diva software.

Biochemical analysis

B and T cell blasts and DCs were sonicated in 25 mM TBS, pH 7.4, containing 1% Triton X-100. Protein concentration was determined by Bradford protein assay. Specific enzyme activities for CtsB and CtsL were measured by incubating 4 µg of cellular protein with Z-Phe-Arg-AMC substrate (50 µM; Bachem) in reaction buffer (50 mM sodium acetate, 8 mM EDTA, and 8 mM DTT, pH 6.0) for 15 min at 37°C, followed by determination of fluorescence (excitation 380 nm; emission 442 nm). In parallel, incubation was performed in the presence of specific CtsL inhibitor (SID26681509; 1 µM) or CtsB inhibitor (CA-074Me, 5 µM), and the subtracted values were calculated as CtsB or CtsL activities, respectively. The activities of βHex, βGal, αFuc, and αMan were assayed in Triton X-100–containing cell lysates (5–50 µg of protein) by estimation of the absorbance of *p*-nitrophenol at 405 nm liberated from the hydrolase-specific monosaccharide substrates incubated in 50 mM sodium citrate buffer, pH 4.6, 0.1% Triton X-100, and 0.4% BSA for 1–16 h at 37°C. The reaction was stopped by addition of 0.4 M glycine/NaOH buffer, pH 10.4 (Kollmann et al., 2012). For the Western blot of CD74 and CtsS, 20 µg of cellular protein were solubilized and separated by 12.5% Tris-Tricine SDS-PAGE to improve the resolution in low-molecular mass range (Schägger, 2006). For the Lamp1 and CtsZ immunoblot, 10 µg of cellular protein were separated by standard 10% Tris-Glycine SDS-PAGE. After transfer of proteins, the membrane was blocked by 1% BSA in TBS and incubated with primary antibodies: rat anti–mouse CD74 (In-1; 1:10,000; BD); goat anti–rat CtsS (M-19; 1:200; Santa Cruz Biotechnology, Inc.); rabbit anti–human GAPDH (FL-335; 1:1,000; Santa Cruz Biotechnology, Inc.); rat anti–mouse Lamp1 (1D4B; 1:250; Developmental Studies Hybridoma Bank); and goat anti–mouse CtsZ (1:200; R&D Systems). After incubation with HRP-conjugated secondary antibodies, immunoreactive bands were detected by enhanced chemiluminescence. Stripping of antibodies from membranes was performed with 0.2 M NaOH for 20 min at RT.

Microscope image acquisition

For ultrastructural analysis, B cell blasts obtained with LPS stimulation for 3 d or BM-DCs were fixed with 4% PFA and 1% glutaraldehyde in 0.1 M of phosphate buffer, pH 7.4. Thereafter they were rinsed and spun down at 1,000 *g* three times in 0.1 M sodium cacodylate buffer, pH 7.2–7.4, and osmicated using 1% osmium tetroxide (Science Services) in the same buffer. After osmication, the cells were dehydrated using ascending ethyl alcohol concentration steps, followed by two rinses in propylene oxide. Infiltration of the embedding medium was performed by immersing the pellets in a 1:1 mixture of propylene oxide and Epon and finally in neat Epon. Ultrathin sections (60 nm) were examined in an electron microscope (EM902; Carl Zeiss). Pictures were taken with a MegaView III digital camera and iTEM software (TRS). For quantitation of cells containing lysosomal storage material, each 100 WT and MLII B cells were evaluated for the presence of both electron-lucent vacuoles and multi-lamellar bodies.

Antigen uptake and degradation assay

Purified splenic B cells stimulated with LPS for 2 d and DCs were incubated with Alexa Fluor 647–conjugated Ova (200 µg/ml and 100 µg/ml, respectively; Life Technologies) and DQ-conjugated Ova (200 µg/ml and 100 µg/ml, respectively; Life Technologies). After 20-min incubation, Ova-loaded cells were washed twice with PBS and chased with Ova-free complete medium. At each time point, cells were immediately moved on ice, washed twice with PBS, and fixed with PBS with 1% PFA. Intracellular fluorescence was measured by flow cytometry.

Antigen presentation assay

Purified splenic B cells stimulated with LPS for 2 d and DCs were incubated with 5, 1, 0.2, and 0.04 mg/ml of chicken Ova or 10^{-5}, 10^{-6}, 10^{-7}, and 10^{-8} M of $Ova_{324–340}$ peptide for 2 h at 37°C and then washed three times. Ova-specific CD4 T cells were purified from OT-II mice and stained with carboxyfluorescein succinimidyl ester (CFSE). 10^5, 0.3×10^5, 0.1×10^5, and 0.03×10^5 Ova-loaded B cells or DCs (from WT or MLII mice) and 10^5 Ova-specific CD4 T cells (from OT-II mice) were coincubated for 4 d on a 96-well plate and investigated with flow cytometry after staining with surface markers. Proliferation of CD4 T cells was measured either by determining the number of CD4 T cells in flow cytometry with the help of count beads or by assessing the decrease of CFSE staining on CD4 T cells. Both measurements gave comparable results. In the same samples, CD19 and CD138 expression of B cells were determined by flow cytometry.

T cell stimulation and cytokine determination

TNF and IFN-γ production by T cells was determined after stimulation with 50 ng/ml phorbol 12-myristate 13-acetate and 1 µM ionomycin in the presence of 10 µg/ml brefeldin A for 4 h at 37°C. After fixation and permeabilization, intracellular TNF and IFN-γ were quantified by flow cytometry.

Immunoglobulin quantification

ELISA for total IgM and IgG in mice serum were performed by sandwich ELISA. 96-well plates were coated with goat anti–mouse IgG (H+L) antibody (1.3 µg/ml; Dianova) followed by blocking with 1% BSA. Sequentially diluted mouse sera (1:1,000–1:150,000) were applied to the plates. Plates were washed and Ig binding was detected by HRP-conjugated antibodies: goat anti–mouse IgM µ-chain (EMD Millipore) and goat anti–mouse IgG γ-chain (EMD Millipore). ELISA for Ova-specific antibodies in mouse serum was performed by indirect ELISA. Plates were coated with Ova (5 µg/ml in 0.1 M $NaHCO_3$, pH 8.2) followed by blocking with 1% BSA. Diluted serum samples (1:4,000) were applied on the plate and detected by HRP-conjugated antibodies: goat anti–mouse IgM µ-chain (EMD Millipore); goat anti–mouse IgG γ-chain (EMD Millipore); goat anti–mouse IgG1 γ1-chain (SouthernBiotech); and rabbit anti–mouse IgG2b γ2b-chain (Invitrogen). Enzyme reaction was done with 3,3′,5,5′-Tetramethylbenzidine substrate (Sigma-Aldrich) and stopped with 0.5 M H_2SO_4, and absorbance was measured by plate reader (VICTOR3; Perkin Elmer) at 450 nm.

IL-6 quantification

Spleen cells (4×10^5 cells in 200 µl of medium per well) from mice were stimulated with hamster anti–mouse CD3 mAb on 96-well plates. After 24 h, culture supernatant was collected and IL-6 was quantified with IL-6 ELISA kit (R&D Systems) according to the manufacturer's protocol.

Mixed lymphocyte reaction

Mixed lymphocyte from spleens of WT and MLII mice ($H\text{-}2^b$) were stimulated with irradiated spleen cells from BALB/c mice ($H\text{-}2^d$) in the presence of IL-2 (10 U/ml). After 5 d, living cells (i.e., effectors) were purified and mixed with CFSE-labeled A20 cells ($H\text{-}2^d$; i.e., targets) for 4 h in different ratios. Living A20 cells were determined by flow cytometry (gated by CFSE and scatter) and counted with the help of count beads. Percent kill was calculated with the following formula: [(number of targets in cultures without effectors − number of targets in cultures with effectors)/number of targets in cultures without effectors] × 100.

Statistical analysis

Data of at least three independent experiments were used for statistical analysis. Statistical significance was calculated by Student's *t* test. Error bars represent SEM.

Online supplemental material

Fig. S1 shows the composition of immune cells in the spleen of WT and MLII mice. Table S1 contains data of flow cytometric subset analysis of lymphocytes in MLII patients. Table S2 contains data on mutations in the *GNPTAB* gene; antibody responses to vaccination; and basal IgG, IgA, and IgM concentrations in serum of four MLII patients. Online supplemental material is available at http://www.jcb.org/cgi/content/full/jcb.201407077/DC1. Additional data are available in the JCB DataViewer at http://dx.doi.org/10.1083/jcb.201407077.dv.

We are grateful to Elizabeth F. Neufeld, Hidde L. Ploegh, Juan S. Bonifacino, and Paul Saftig for critical discussions and comments of the manuscript. We also thank J. Brand and C. Raithore for technical assistance.

This work was supported by grants from the Japan Society for the Promotion of Science (JSPS Postdoctoral Fellowships for Research Abroad to T. Otomo) and Deutsche Forschungsgemeinschaft (FOR885 to K. Kollmann; MI 476/3, SFB841, and KFO228 to H.-W. Mittrücker; and Fritz Thyssen Foundation to T. Braulke).

The authors declare no competing financial interests.

Submitted: 17 July 2014
Accepted: 8 December 2014

References

Bao, M., B.J. Elmendorf, J.L. Booth, R.R. Drake, and W.M. Canfield. 1996. Bovine UDP-N-acetylglucosamine:lysosomal-enzyme *N*-acetylglucosamine-1-phosphotransferase. II. Enzymatic characterization and identification of the catalytic subunit. *J. Biol. Chem.* 271:31446–31451. http://dx.doi.org/10.1074/jbc.271.49.31446

Barnden, M.J., J. Allison, W.R. Heath, and F.R. Carbone. 1998. Defective TCR expression in transgenic mice constructed using cDNA-based α- and β-chain genes under the control of heterologous regulatory elements. *Immunol. Cell Biol.* 76:34–40. http://dx.doi.org/10.1046/j.1440-1711.1998.00709.x

Braulke, T., and J.S. Bonifacino. 2009. Sorting of lysosomal proteins. *Biochim. Biophys. Acta*. 1793:605–614. http://dx.doi.org/10.1016/j.bbamcr.2008.10.016

Braulke, T., A. Raas-Rothschild, and S. Kornfeld. 2013. I-Cell Disease and Pseudo-Hurler Polydystrophy: Disorders of Lysosomal Enzyme Phosphorylation and Localization. *In* The Online Metabolic and Molecular Bases of Inherited Disease. D. Valle, A.L. Beaudet, B. Vogelstein, K.W. Kinzler, S.E. Antonarakis, A. Ballabio, C. Scriver, B. Childs, W. Sly, F. Bunz, K.M. Gibson, G. Mitchell, editors. McGraw Hill, New York. Chapter 138.

Comans-Bitter, W.M., R. de Groot, R. van den Beemd, H.J. Neijens, W.C. Hop, K. Groeneveld, H. Hooijkaas, and J.J. van Dongen. 1997. Immunophenotyping of blood lymphocytes in childhood. Reference values for lymphocyte subpopulations. *J. Pediatr.* 130:388–393. http://dx.doi.org/10.1016/S0022-3476(97)70200-2

Daly, T.M., R.G. Lorenz, and M.S. Sands. 2000. Abnormal immune function in vivo in a murine model of lysosomal storage disease. *Pediatr. Res.* 47:757–762. http://dx.doi.org/10.1203/00006450-200006000-00012

Delamarre, L., M. Pack, H. Chang, I. Mellman, and E.S. Trombetta. 2005. Differential lysosomal proteolysis in antigen-presenting cells determines antigen fate. *Science*. 307:1630–1634. http://dx.doi.org/10.1126/science.1108003

Delamarre, L., R. Couture, I. Mellman, and E.S. Trombetta. 2006. Enhancing immunogenicity by limiting susceptibility to lysosomal proteolysis. *J. Exp. Med.* 203:2049–2055. http://dx.doi.org/10.1084/jem.20052442

Desnick, R.J., H.L. Sharp, G.A. Grabowski, R.D. Brunning, P.G. Quie, J.H. Sung, R.J. Gorlin, and J.U. Ikonne. 1976. Mannosidosis: clinical, morphologic, immunologic, and biochemical studies. *Pediatr. Res.* 10:985–996. http://dx.doi.org/10.1203/00006450-197612000-00008

Donaldson, J.G., D. Finazzi, and R.D. Klausner. 1992. Brefeldin A inhibits Golgi membrane-catalysed exchange of guanine nucleotide onto ARF protein. *Nature*. 360:350–352. http://dx.doi.org/10.1038/360350a0

Driessen, C., R.A. Bryant, A.M. Lennon-Duménil, J.A. Villadangos, P.W. Bryant, G.P. Shi, H.A. Chapman, and H.L. Ploegh. 1999. Cathepsin S controls the trafficking and maturation of MHC class II molecules in dendritic cells. *J. Cell Biol.* 147:775–790. http://dx.doi.org/10.1083/jcb.147.4.775

Fairfax, K.A., A. Kallies, S.L. Nutt, and D.M. Tarlinton. 2008. Plasma cell development: from B-cell subsets to long-term survival niches. *Semin. Immunol.* 20:49–58. http://dx.doi.org/10.1016/j.smim.2007.12.002

Fratantoni, J.C., C.W. Hall, and E.F. Neufeld. 1969. The defect in Hurler and Hunter syndromes. II. Deficiency of specific factors involved in mucopolysaccharide degradation. *Proc. Natl. Acad. Sci. USA*. 64:360–366. http://dx.doi.org/10.1073/pnas.64.1.360

Furuta, K., E. Walseng, and P.A. Roche. 2013. Internalizing MHC class II–peptide complexes are ubiquitinated in early endosomes and targeted for lysosomal degradation. *Proc. Natl. Acad. Sci. USA*. 110:20188–20193. http://dx.doi.org/10.1073/pnas.1312994110

Glickman, J.N., and S. Kornfeld. 1993. Mannose 6-phosphate–independent targeting of lysosomal enzymes in I-cell disease B lymphoblasts. *J. Cell Biol.* 123:99–108. http://dx.doi.org/10.1083/jcb.123.1.99

Griffiths, G.M., and S. Isaaz. 1993. Granzymes A and B are targeted to the lytic granules of lymphocytes by the mannose-6-phosphate receptor. *J. Cell Biol.* 120:885–896. http://dx.doi.org/10.1083/jcb.120.4.885

Honey, K., and A.Y. Rudensky. 2003. Lysosomal cysteine proteases regulate antigen presentation. *Nat. Rev. Immunol.* 3:472–482. http://dx.doi.org/10.1038/nri1110

Inaba, K., W.J. Swiggard, R.M. Steinman, N. Romani, G. Schuler, and C. Brinster. 2009. Isolation of dendritic cells. *Curr. Protoc. Immunol.* Chapter 3:Unit 3.7.

Karageorgos, L.E., E.L. Isaac, D.A. Brooks, E.M. Ravenscroft, R. Davey, J.J. Hopwood, and P.J. Meikle. 1997. Lysosomal biogenesis in lysosomal storage disorders. *Exp. Cell Res.* 234:85–97. http://dx.doi.org/10.1006/excr.1997.3581

Kojima, S., S. Okada, H. Kai, K. Ha, O. Nose, T. Ikeda, T. Yutaka, M. Kato, and H. Yabuuchi. 1979. A case of mucolipidosis II: Biochemical, nutritional, and immunological studies. *Brain Dev.* 1:26–30. http://dx.doi.org/10.1016/S0387-7604(79)80031-5

Kollmann, K., M. Damme, S. Markmann, W. Morelle, M. Schweizer, I. Hermans-Borgmeyer, A.K. Röchert, S. Pohl, T. Lübke, J.C. Michalski, et al. 2012. Lysosomal dysfunction causes neurodegeneration in mucolipidosis II 'knock-in' mice. *Brain.* 135:2661–2675. http://dx.doi.org/10.1093/brain/aws209

Kollmann, K., J.M. Pestka, S.C. Kühn, E. Schöne, M. Schweizer, K. Karkmann, T. Otomo, P. Catala-Lehnen, A.V. Failla, R.P. Marshall, et al. 2013. Decreased bone formation and increased osteoclastogenesis cause bone loss in mucolipidosis II. *EMBO Mol. Med.* 5:1871–1886. http://dx.doi.org/10.1002/emmm.201302979

Kudo, M., M. Bao, A. D'Souza, F. Ying, H. Pan, B.A. Roe, and W.M. Canfield. 2005. The α- and β-subunits of the human UDP-*N*-acetylglucosamine: lysosomal enzyme *N*-acetylglucosamine-1-phosphotransferase [corrected] are encoded by a single cDNA. *J. Biol. Chem.* 280:36141–36149. http://dx.doi.org/10.1074/jbc.M509008200

Little, L., M. Alcouloumre, A.M. Drotar, S. Herman, R. Robertson, R.Y. Yeh, and A.L. Miller. 1987. Properties of *N*-acetylglucosamine 1-phosphotransferase from human lymphoblasts. *Biochem. J.* 248:151–159.

Ma, J.K., M.Y. Platt, J. Eastham-Anderson, J.S. Shin, and I. Mellman. 2012. MHC class II distribution in dendritic cells and B cells is determined by ubiquitin chain length. *Proc. Natl. Acad. Sci. USA.* 109:8820–8827. http://dx.doi.org/10.1073/pnas.1202977109

Malm, D., D.S. Halvorsen, L. Tranebjaerg, and H. Sjursen. 2000. Immunodeficiency in α-mannosidosis: a matched case-control study on immunoglobulins, complement factors, receptor density, phagocytosis and intracellular killing in leucocytes. *Eur. J. Pediatr.* 159:699–703. http://dx.doi.org/10.1007/s004310000545

Maric, M., B. Arunachalam, U.T. Phan, C. Dong, W.S. Garrett, K.S. Cannon, C. Alfonso, L. Karlsson, R.A. Flavell, and P. Cresswell. 2001. Defective antigen processing in GILT-free mice. *Science.* 294:1361–1365. http://dx.doi.org/10.1126/science.1065500

Morbach, H., E.M. Eichhorn, J.G. Liese, and H.J. Girschick. 2010. Reference values for B cell subpopulations from infancy to adulthood. *Clin. Exp. Immunol.* 162:271–279. http://dx.doi.org/10.1111/j.1365-2249.2010.04206.x

Nakagawa, T., W. Roth, P. Wong, A. Nelson, A. Farr, J. Deussing, J.A. Villadangos, H. Ploegh, C. Peters, and A.Y. Rudensky. 1998. Cathepsin L: critical role in Ii degradation and CD4 T cell selection in the thymus. *Science.* 280:450–453. http://dx.doi.org/10.1126/science.280.5362.450

Nakagawa, T.Y., W.H. Brissette, P.D. Lira, R.J. Griffiths, N. Petrushova, J. Stock, J.D. McNeish, S.E. Eastman, E.D. Howard, S.R. Clarke, et al. 1999. Impaired invariant chain degradation and antigen presentation and diminished collagen-induced arthritis in cathepsin S null mice. *Immunity.* 10:207–217. http://dx.doi.org/10.1016/S1074-7613(00)80021-7

Otomo, T., T. Muramatsu, T. Yorifuji, T. Okuyama, H. Nakabayashi, T. Fukao, T. Ohura, M. Yoshino, A. Tanaka, N. Okamoto, et al. 2009. Mucolipidosis II and III α/β: mutation analysis of 40 Japanese patients showed genotype–phenotype correlation. *J. Hum. Genet.* 54:145–151. http://dx.doi.org/10.1038/jhg.2009.3

Owada, M., and E.F. Neufeld. 1982. Is there a mechanism for introducing acid hydrolases into liver lysosomes that is independent of mannose 6-phosphate recognition? Evidence from I-cell disease. *Biochem. Biophys. Res. Commun.* 105:814–820. http://dx.doi.org/10.1016/0006-291X(82)91042-7

Peters, M.E., S. Arya, L.O. Langer, E.F. Gilbert, R. Carlson, and W. Adkins. 1985. Narrow trachea in mucopolysaccharidoses. *Pediatr. Radiol.* 15:225–228. http://dx.doi.org/10.1007/BF02388760

Raas-Rothschild, A., V. Cormier-Daire, M. Bao, E. Genin, R. Salomon, K. Brewer, M. Zeigler, H. Mandel, S. Toth, B. Roe, et al. 2000. Molecular basis of variant pseudo-hurler polydystrophy (mucolipidosis IIIC). *J. Clin. Invest.* 105:673–681. http://dx.doi.org/10.1172/JCI5826

Reitman, M.L., A. Varki, and S. Kornfeld. 1981. Fibroblasts from patients with I-cell disease and pseudo-Hurler polydystrophy are deficient in uridine 5′-diphosphate-*N*-acetylglucosamine: glycoprotein *N*-acetylglucosaminylphosphotransferase activity. *J. Clin. Invest.* 67:1574–1579. http://dx.doi.org/10.1172/JCI110189

Riese, R.J., R.N. Mitchell, J.A. Villadangos, G.P. Shi, J.T. Palmer, E.R. Karp, G.T. De Sanctis, H.L. Ploegh, and H.A. Chapman. 1998. Cathepsin S activity regulates antigen presentation and immunity. *J. Clin. Invest.* 101:2351–2363. http://dx.doi.org/10.1172/JCI1158

Roche, P.A., and P. Cresswell. 1991. Proteolysis of the class II-associated invariant chain generates a peptide binding site in intracellular HLA-DR molecules. *Proc. Natl. Acad. Sci. USA.* 88:3150–3154. http://dx.doi.org/10.1073/pnas.88.8.3150

Saftig, P., and J. Klumperman. 2009. Lysosome biogenesis and lysosomal membrane proteins: trafficking meets function. *Nat. Rev. Mol. Cell Biol.* 10:623–635. http://dx.doi.org/10.1038/nrm2745

Sawkar, A.R., W. D'Haeze, and J.W. Kelly. 2006. Therapeutic strategies to ameliorate lysosomal storage disorders—a focus on Gaucher disease. *Cell. Mol. Life Sci.* 63:1179–1192. http://dx.doi.org/10.1007/s00018-005-5437-0

Schägger, H. 2006. Tricine–SDS-PAGE. *Nat. Protoc.* 1:16–22. http://dx.doi.org/10.1038/nprot.2006.4

Schröder, B.A., C. Wrocklage, A. Hasilik, and P. Saftig. 2010. The proteome of lysosomes. *Proteomics.* 10:4053–4076. http://dx.doi.org/10.1002/pmic.201000196

Stiehm, E.R., and H.H. Fudenberg. 1966. Serum levels of immune globulins in health and disease: a survey. *Pediatrics.* 37:715–727.

Tiede, S., S. Storch, T. Lübke, B. Henrissat, R. Bargal, A. Raas-Rothschild, and T. Braulke. 2005. Mucolipidosis II is caused by mutations in *GNPTA* encoding the α/β GlcNAc-1-phosphotransferase. *Nat. Med.* 11:1109–1112. http://dx.doi.org/10.1038/nm1305

Tsuji, A., K. Omura, and Y. Suzuki. 1988. I-cell disease: evidence for a mannose 6-phosphate independent pathway for translocation of lysosomal enzymes in lymphoblastoid cells. *Clin. Chim. Acta.* 176:115–121. http://dx.doi.org/10.1016/0009-8981(88)90181-7

Waheed, A., R. Pohlmann, A. Hasilik, and K. von Figura. 1981. Subcellular location of two enzymes involved in the synthesis of phosphorylated recognition markers in lysosomal enzymes. *J. Biol. Chem.* 256:4150–4152.

Waheed, A., R. Pohlmann, A. Hasilik, K. von Figura, A. van Elsen, and J.G. Leroy. 1982. Deficiency of UDP-*N*-acetylglucosamine:lysosomal enzyme *N*-acetylglucosamine-1-phosphotransferase in organs of I-cell patients. *Biochem. Biophys. Res. Commun.* 105:1052–1058. http://dx.doi.org/10.1016/0006-291X(82)91076-2